Electronic Supplementary Material (ESI) for RSC Advances.

Electronic supplementary information (ESI)

Light activated non-reciprocal motion in liquid crystalline networks by designed microactuator architecture

Daniele Martella,[‡] *Diego Antonioli,*[‡] *Sara Nocentini, Diederik S. Wiersma, Giancarlo Galli,*
*Michele Laus and Camilla Parmeggiani**

Index

Mesomorphic properties of the mixtures -- *S3*

Table S1. --- *S3*

Figure S1 --- *S4*

Polymerization condition studies by ATR spectroscopy -- *S4*

Figure S2 --- *S5*

Figure S3 --- *S6*

Figure S4 --- *S6*

Penetration length measurement--- *S7*

Table S2 -- *S***Errore. Il segnalibro non è definito.**

Table S3 --- *S7*

Figure S5 --- *S8*

Mesomorphic properties of the mixtures

Table S1. Composition and mesomorphic properties of the monomeric mixtures.

	1[a]	**2**[a]	**3**[a]	**Irgacure 369**[a]	**T_m**[b]**(°C)**	**T_{NI}**[c]**(°C)**
MM10	88%	10%	1%	1%	55	50
MM20	78%	20%	1%	1%	53	57
MM30	68%	30%	1%	1%	46	64
MM40	58%	40%	1%	1%	46	71

[a] Mol % in the total mixture [b] Determined from the peak maximum in the first heating scan of DSC trace. [c] Determined from the peak maximum in the second DSC heating scan.

In the first heating scan, **MM10** and **MM20** melted directly to the isotropic phase whereas a nematic phase was observed for **MM30** and **MM40**. On cooling, all the mixtures displayed the isotropic-nematic transition and the nematic phase was frozen at room temperature. In the second heating scan, a melting endotherm preceded by a cold crystallization exotherm, was observed only for **MM10**, and occurred at temperatures lower than the nematic-isotropic transition. All the other mixtures displayed only the nematic-isotropic transition. The isotropization temperature, T_{NI}, homogeneously determined from the second heating scan**,** increased linearly from 50 to 70°C as the percentage of **2** increases.

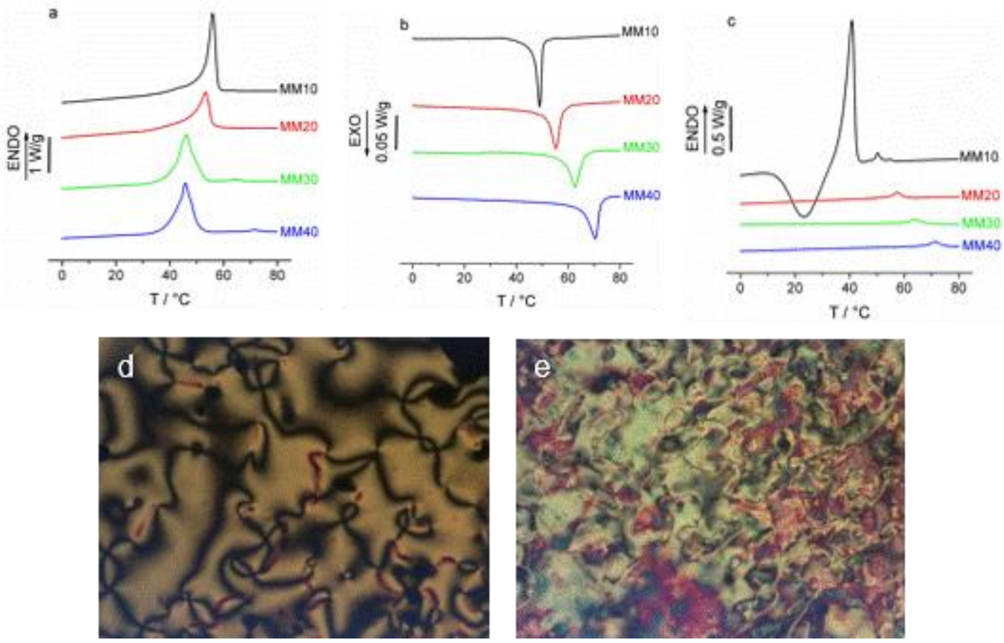

Figure S1. DSC traces and POM images of monomeric mixtures. DSC traces recorded at 10 °C/min related to the first heating (a), first cooling (b) and second heating (c). POM image of **MM20** at 50 °C (e). The image shows the typical nematic schlieren textures with 2-brush and 4-brush defects. After some hours at room temperature, crystallization is not observed in the same mixture f).

Polymerization condition studies by ATR spectroscopy

The polymerization process of macroscopic films was monitored by means of ATR spectroscopy. The process was study at room temperature and 45 °C (some degree below the T_{NI}). Cells were irradiated with an UV lamp for different times, then opened and analyzed by ATR. **Figure S2** reports the results for the mixtures **MM20**. The absorbance signal at 1639 cm^{-1}, due to the C=C stretching vibration of the acrylate groups, progressively weakened with irradiation time. 5 second irradiation was enough to obtain an easily handle film for both temperatures. However, after 10 minutes of irradiation, residual acrylate peak was observed in both cases indicating that the polymerization process was arrested before its completion. This could be attributed to the increased viscosity of the film limiting the diffusion on the unreacted acrylate groups and radicals. To further increase the polymerization degree, temperature was increased up to 65 °C and the film irradiated for further 10 minutes. While in the film polymerized in the first step at room temperature, the acrylate peak is still detectable, it was completely disappeared for the film polymerized first at 45 °C.

Polymerization process for the other mixtures proceed in a very similar way, even if the higher crosslinking percentage lead to a slightly less final conversion degree as indicate by a very small residual acrylate peak.

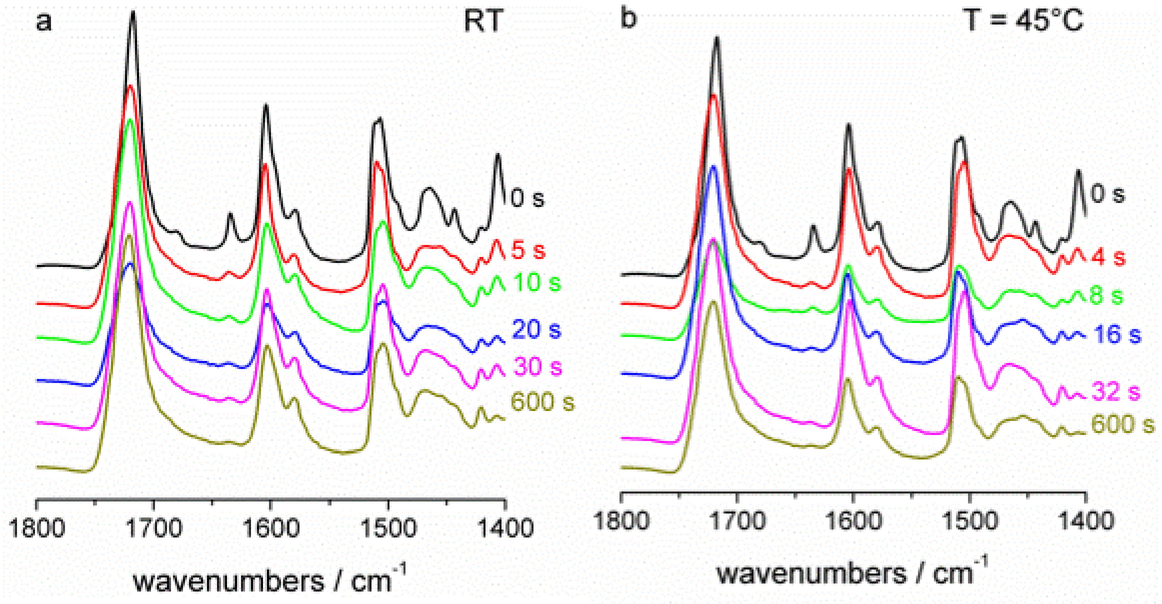

Figure S2. ATR spectra for MM20 polymerization. a) polymerization at RT. Graph related to irradiation time (from up to down) 0 sec, 5 sec, 10 sec, 20 sec, 30 sec, 600 sec plus post polymerization at 65 °C; b) polymerization at 45°C: spectra related to irradiation time (from up to down) 0 sec, 4 sec, 8 sec, 16 sec, 32 sec, 600 sec, 600 sec and post polymerization at 65 °C.

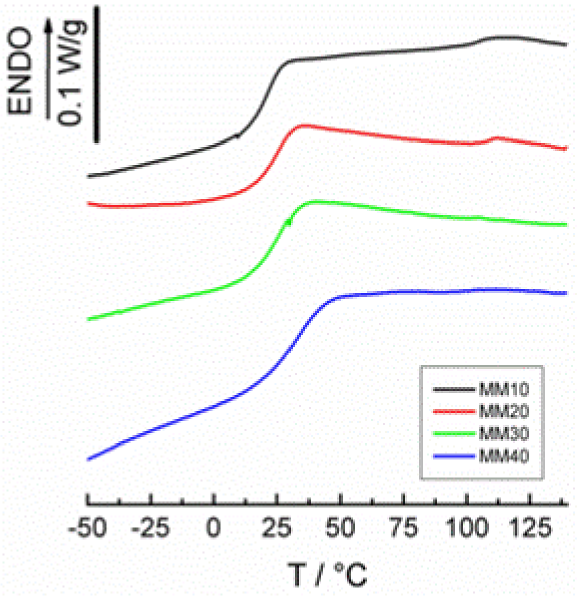

Figure S3. DSC second heating run (10°/min) of the films from mixtures **MM10-MM40.**

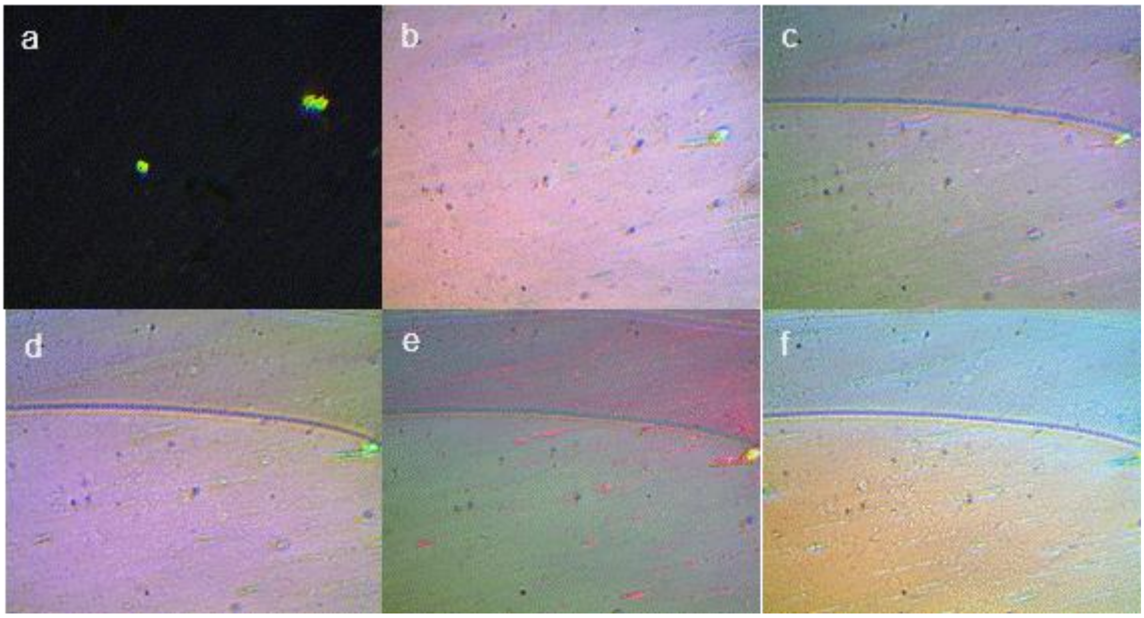

Figure S4. POM images of film **MM20** on heating at: a) room temperature; b) same image recorded with the sample rotated of 45° in respect of the analyzer; c) image recorded heating the sample at 80 °C; d) image recorded heating the sample at 100 °C; e) image recorded heating the sample at 125 °C; f) image recorded heating the sample at 150 °C. Images c) - f) were observed with 45° in respect to the analyzer.

Penetration depth measurement

To evaluate the penetration length of the different mixtures, we shined a 20 µm thick film with a green laser (532 nm). Comparing the laser intensity that pass through the film with the value that we measured before the LCE film, we can establish the penetration length. We estimate to be 6 µm for the different mixtures. No differences in fact are expected in absorption varying the cross-linker density.

Table S2. Light response of LCN macrostripes. Bending (**t_b**), relaxation (**t_r**) times and related average angular speed (**v**) for the stripes under different excitation powers.

	2.87 mW		**4.19 mW**		**5.89 mW**		**8.27 mW**	
	t_b (s) (v deg/s)	**t_r (s) (v deg/s)**	**t_b (s) (v deg/s)**	**t_r (s) (v deg/s)**	**t_b (s) (v deg/s)**	**t_r (s) (v deg/s)**	**t_b (s) (v deg/s)**	**t_r (s) (v deg/s)**
MM10	2.5 (20)	1.8 (28)	2.9 (40)	2.2 (52)	1.9 (84)	1.9 (84)	2.2 (82)	2.2 (82)
MM20	4.5 (4)	1.5 (13)	2.3 (22)	0.9 (55)	1.5 (100)	1.0 (150)	0.5 (360)	0.9 (200)
MM30	1.7 (6)	0.6 (17)	2.0 (15)	0.8 (37.5)	1.4 (36)	1.1 (15)	0.7 (157)	1.3 (85)
MM40	1.2 (8)	0.9 (11)	1.3 (12)	1.3 (12)	1.0 (20)	1.0 (20)	0.9 (111)	1.3 (77)

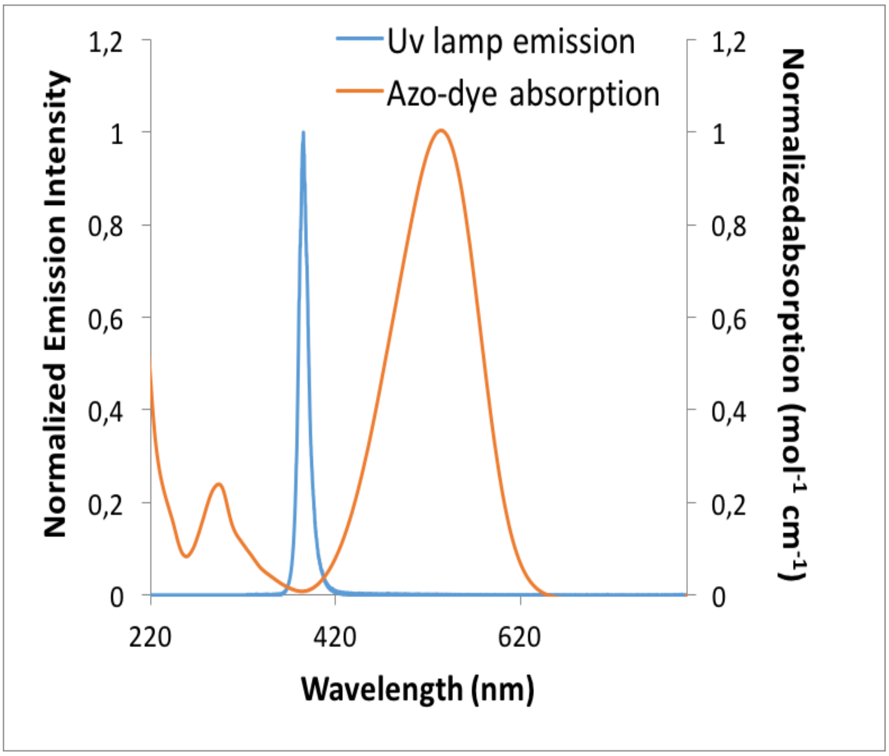

Figure S5. Lamp and dye absorption spectra